Monthly Notices of the ROYAL ASTRONOMICAL SOCIETY
MNRAS **457,** 3115–3118 (2016) doi:10.1093/mnras/stw196

# In-lab ALOHA mid-infrared up-conversion interferometer with high fringe contrast @$\lambda = 3.39$ μm

L. Szemendera,[1⋆] P. Darré,[1] R. Baudoin,[1] L. Grossard,[1⋆] L. Delage,[1] H. Herrmann,[2] C. Silberhorn[2] and F. Reynaud[1]

[1]*Xlim, Département Photonique, Université de Limoges, UMR CNRS 7252, 123 Av. Albert Thomas, F-87060 Limoges CEDEX, France*
[2]*Universität Paderborn, Angewandte Physik, Warburger Str. 100, D-33098 Paderborn, Germany*

Accepted 2016 January 20. Received 2016 January 8; in original form 2015 November 13

## ABSTRACT

We report on the implementation of a mid-infrared (MIR) interferometer prototype for furthermore application in the framework of high-resolution imaging in astronomy. This paper demonstrates the possibility to extend to the *L* band our experimental study performed on the up-conversion interferometer in *H* band. This in-laboratory preliminary experiment allowed us to get the first fringes with the MIR Astronomical Light Optical Hybrid Analysis (ALOHA) @3.39 μm up-conversion interferometer with a bright quasi monochromatic source (HeNe 3.39 μm). A stable contrast greater than 98 per cent has been reached. This opens the possibility to propose an alternative instrument for the demanding domain of high resolution imaging in the MIR domain.

**Key words:** instrumentation: interferometers – techniques: interferometric.

## 1 INTRODUCTION

In the general framework of thermal infrared investigation, the mid-infrared (MIR) and far-infrared domains address several prominent scientific areas, such as protoplanetary discs study (Gräfe & Wolf 2013). When focusing on the scope of high-resolution imaging in astronomy, the interferometers able to produce data in the *L*, *M* and *N* bands, such as MATISSE, VISIR or MIDI, are working with very low flux (Lopez et al. 2009), and undergo thermal noise emitted by the whole components included in the long instrumental chain (Perrin et al. 2001).

In such a telescope array, each interferometric arm can involve more than 20 mirrors. At room temperature, the thermal emission of the mirror train can easily exceed the astronomical signal, significantly reducing the limiting magnitude. In a classical instrument, this requires the use of a chopped and nodded detection modes and its related data processing.

In order to limit the impact of this main noise contribution, the ALOHA (Astronomical Light Optical Hybrid Analysis) instrument implements a hybrid interferometer where the astronomical light is frequency shifted into the near-infrared domain through a sum frequency generation (SFG) process (Boyd 1990). The MIR signal is converted out of the thermal infrared domain as close as possible to the telescope focus. This way, the main part of the instrumental chain is not subject to any thermal noise disturbance.

Moreover, ALOHA addresses at the same time spatial filtering and polarization issues. The up-conversion stage is operated in a spatially single-mode experimental configuration leading to a first spatial filtering stage and a polarization mode selection. Hence, shifting the star light spectrum to the near-infrared domain allows us to implement an all-fibred, polarization maintaining instrument with an accurate control of the spatial and polarization behaviours, mandatory for a good fringe contrast calibration.

In a previous work, we investigated the joint use of SFG and high-resolution imaging by spatial coherence analysis (Brustlein et al. 2008) at 1550 nm down to the photon counting regime (Gomes et al. 2014). This spectral domain was chosen for the sake of technological constrains. This current paper demonstrates the extension of the ALOHA scope to the MIR spectral domain and reports the first high-flux fringes obtained with the up-conversion interferometer @3.39 μm.

## 2 PRINCIPLE OF THE MIR ALOHA UP-CONVERSION INTERFEROMETER

Fig. 1 gives a schematic view of the MIR ALOHA up-conversion interferometer. The telescope array collects the MIR light from the astronomic target. In each interferometric arm, the optical field is converted in a non-linear crystal through an SFG process towards the near-infrared domain. This way, all over the downstream optical path, it is possible to use mature guided-wave components available for the telecommunication spectral window, and silicon detectors.

The SFG stages allow us to shift the spectrum of the source from the MIR to the near-infrared spectral domain. SFG is a second-order non-linear process which allows us to merge a signal photon at frequency $\nu_s$ with a pump photon $\nu_p$ in order to generate a converted one at $\nu_c$. This process is known to be inherently noiseless

⋆ E-mail: ludovic.szemendera@unilim.fr (LS); ludovic.grossard@unilim.fr (LG)

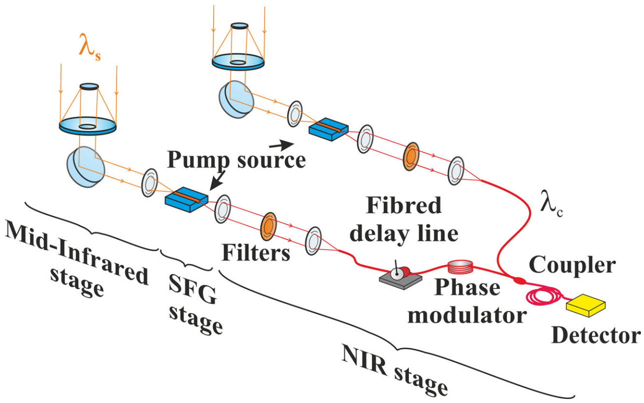


**Figure 1.** Scheme of the ALOHA instrument on site. In each arm of the interferometer, the MIR fields coming from the astronomical source are shifted to the NIR domain through an SFG process, and then mixed to generate a fringe pattern in the time domain.

(Louisell et al. 1961), at the cost of a moderate conversion efficiency. This can be intuitively understood as the generation of a converted photon requires an input astronomical photon. The frequency of the converted photon can be inferred by the energy conservation law:

$$h\nu_c = h\nu_p + h\nu_s.$$

On the other hand, the SFG process efficiency depends on the quasi-phase-matching condition between the two interacting waves and the generated one. This reflects the ability of the locally generated waves to interact constructively in the non-linear medium during propagation. It results in a spectral selectivity theoretically described in reference, Boyd (1990).

At the output of each crystal, a spectral filtering is applied in order to reject the pump and undesirable signals residues. The converted light is then launched into optical fibres and guided-wave components to be processed. These devices are polarization maintaining, and single-mode in order to ensure the spatial filtering. Fibred delay lines are implemented on each arm to set the zero optical path difference in the interferometer. A fibre piezoelectric module allows us to induce a temporal modulation of the optical path difference in order to display the interferometric fringes as function of time. A single-mode fibre coupler allows us to mix the two converted fields with an optimum spatial overlapping. The output interferometric signal is then detected with a silicon detector.

## 3 MIR SFG INTERFEROMETER IN-LAB EXPERIMENTAL SETUP AND RESULTS

The in-lab version of the MIR ALOHA up-conversion interferometer has been designed using an artificial input source. Thus, the experimental setup is based on a Mach Zehnder architecture, and aims to test the possibility to operate such an instrument in the *L* astronomical band. The guided components are single mode and polarization maintaining all over the interferometric arms, including the non-linear stage.

The experimental scheme of ALOHA @3.39 µm prototype is shown in Fig. 2. The input stage mimics the telescope assembly and provides two coherent beams to feed the two interferometric arms. The signal source comes from a quasi-monochromatic Continuous Wave HeNe laser emitting at 3.39 µm.

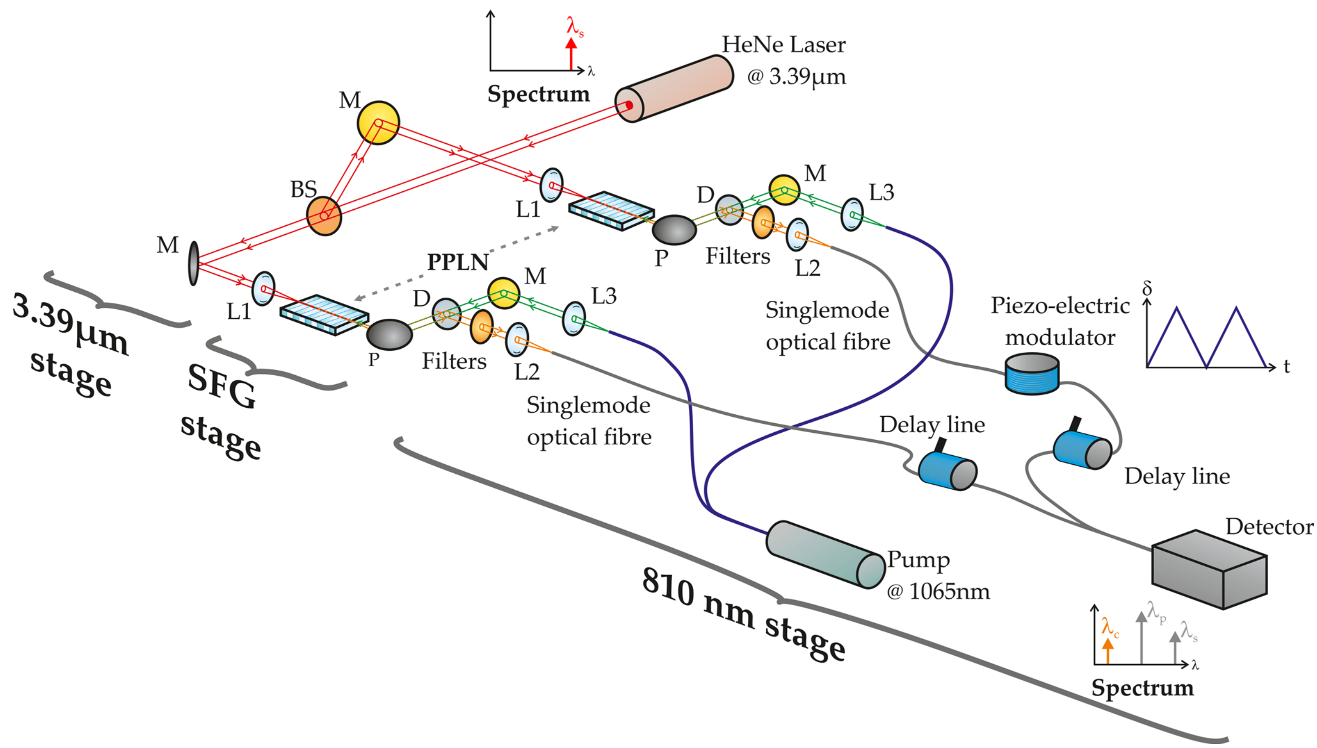


**Figure 2.** Description of the experimental setup. M: injection mirrors for the infrared signal at 3.39 µm; L1: focusing lens for the MIR injection into the Periodically Poled Lithium Niobate (PPLN) waveguide; L2: focusing lens for the converted signal into a fibre single mode at 810 nm; L3: collimating lens for the pump signal; P: off-axis parabola; D: dichroic mirror used to separate converted signal from pump signal; BS: beam splitter used to separate the MIR signal in two separated ways.

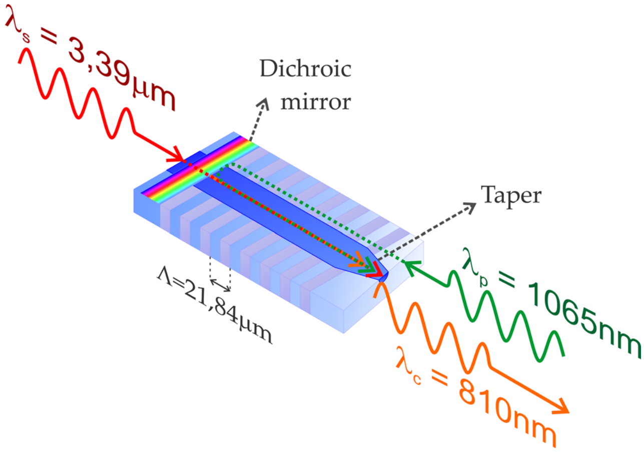


**Figure 3.** PPLN injection scheme. The pump wave at 1065 nm propagates in the reverse direction, and is coupled into the waveguide thanks to a taper. After a back-reflection by a dichroic mirror, the pump field interacts with the signal at 3.39 μm to generate the converted wave at 810 nm.

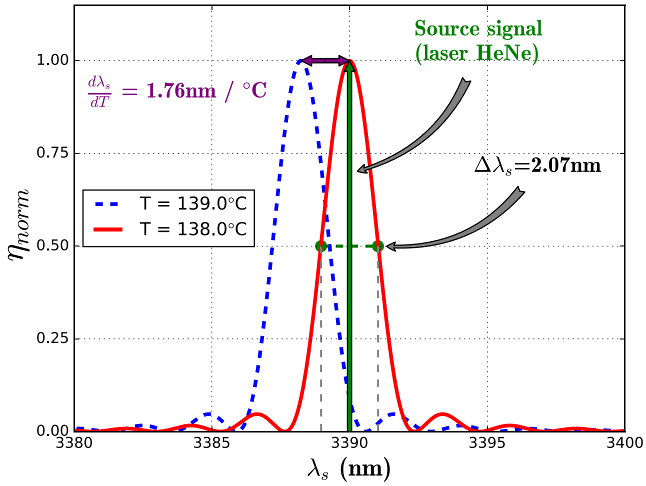


**Figure 4.** Normalized conversion efficiency curve versus the signal wavelength. This curve has been computed with the following parameters: polling period: $\Lambda = 21.84$ μm, pump signal: $\lambda_p = 1065$ nm. The main curve is for a crystal temperature at $T = 139.0$°C, the dotted curve is at $T = 138.0$°C. The source signal is a Dirac at $\lambda_s = 3.39$ μm. The PPLN length is $L = 92$ mm.

The 3.5 mW signal is shared equally between the two interferometric arms thanks to a pellicle beam splitter BS. Over the MIR stage, a set of mirrors and objectives allow the injection of the signal into frequency converters in each arm. These converters consist of periodically poled Ti-indiffused waveguides in $LiNbO_3$. The waveguides are designed to provide low-loss single-mode guiding in the MIR range. Poling periods around 22 μm enable the phase-matching for the SFG process. The entire length of the non-linear conversion section is 92 mm.

The non-linear stages are powered by a distributed feedback laser laser emitting at 1065 nm to generate a wave at 810 nm through the SFG process. On each interferometric arm, the maximum power conversion efficiency is measured in the range of $3{\cdot}10^{-5}$ when each non-linear crystal is powered by a 60 mW pump power. Notice that this overall throughput includes the non-linear efficiency and the whole losses resulting from the launching and collimating stages, including the stringent spatial filtering. This current low conversion efficiency is to be improved for future application, e.g. by using pigtailed techniques as demonstrated by Büchter (Büchter, Herrmann & Sohler 2011)

The pump signal is injected backward using a taper, and is then back-reflected towards the output of the Periodically Poled Lithium Niobate (PPLN) waveguide thanks to a dichroic mirror directly deposited at the waveguide endface [Anti-Reflection (AR) at 3.39 μm and High-Reflection (HR) at 1065 nm, see Fig. 3]. The waveguide taper allows us to ensure a better control of the pump beam geometry leading to the optimal spatial overlapping in the non-linear crystals between the pump at 1065 nm and the signal at 3.39 μm.

We define the normalized conversion efficiency curve of the SFG process as the ratio between the converted power and the signal one as a function of the signal wavelength. This curve depends on the crystal's optical and geometrical parameters (Fig. 4) and can be tuned by a fine control of its temperature. The full width at half-maximum of the conversion efficiency curve defines the spectral acceptance $\Delta\lambda_s$. In our experimental configuration, $\Delta\lambda_s = 2$ nm whereas the He–Ne signal has a subpicometre single line spectrum. The two non-linear crystals are placed in thermally regulated enclosures. Their temperatures are matched with an accuracy of 0.1°C to centre the conversion efficiency curves on the He–Ne line, such that the conversion efficiency is optimized on each arm of the interferometer.

In each arm of the interferometer, the converted wave at the output of the PPLN crystal is spectrally cleaned up through a notch filter to reject the unwanted pump residue and its second harmonic. The converted beam is then spatially filtered over a 4 m polarization maintaining optical fibre, single-mode at 810 nm. The control of the polarization state and spatial quality of the converted beams are mandatory to get a stable and well-calibrated interferometric signal. A fibre delay line is inserted on each arm of the interferometer to operate near the zero optical path difference. Note that the delay line setting is not crucial in this experimental configuration since the converted wave is quasi-monochromatic. However, with a broadband signal @3.39 μm, an accurate delay line setting would be necessary. In this case, the coherence length of the converted field depends directly on the spectral acceptance bandwidth of the PPLN ($\Delta\lambda_s = 2$ nm) and would be equal to 5.6 mm.

On one arm of the interferometer, a high-voltage wave generator (±150 V) drives a fibre optical path modulator with a triangular voltage function to display the fringe pattern as a function of time. The interferometric recombination of the two converted waves is achieved through a single-mode polarization maintaining coupler. The resulting fringe pattern is then detected by a classical Avalanche photodiode (APD) silicon detector coupled via an analogue-to-digital converter to an acquisition device enabling the data processing.

Fig. 5 shows the fringe pattern recorded at the output of the up-conversion interferometer as a function of time over a single 100 ms long frame. The fringe contrast of each frame is computed from the ratio of the modulation and the DC peaks of its spectral power density. This contrast value is unbiased from the photometric imbalance between our two interferometric arms. The fringes and photometric measurements are acquired successively. The main error results from the intensity fluctuation in each interferometric arm (in the range of 10 per cent) and the non-real-time photometric correction.

The average contrast experimentally measured is equal to $C = 98$ per cent with a standard deviation of $\sigma = 4$ per cent over a set of 1500 frames. The high experimental contrast (close to 100 per cent) demonstrates a very good control on each step of our interferometer: non-linear processes, spatial and polarization behaviours.

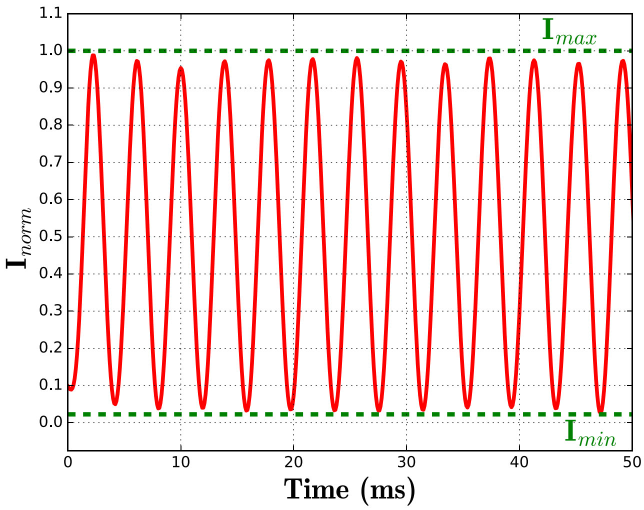


**Figure 5.** Experimental high-flux temporal fringes recorded at the output of the ALOHA@3.39 µm interferometer.

## 4 CONCLUSION AND PERSPECTIVES

We have experimentally demonstrated the possibility to implement an up-conversion interferometer in the MIR at 3.39 µm. This preliminary experiment has been conducted in the high-flux regime and confirms the possibility to use an SFG stage on each arm of an interferometer dedicated to high resolution imaging in the *L* band. We have obtained a very high fringe contrast, equal to 98 per cent thanks to polarization maintaining single mode fibres. Our next investigations will focus on the photon counting regime by attenuating the input signal monochromatic flux and addressing faint broad-band sources to fit the astronomical requirement.


## ACKNOWLEDGEMENTS

This work has been financially supported by the Centre National d'Études Spatiales (CNES), the Institut National des Sciences de l'Univers (INSU), Airbus Group, Thales Alenia Space and the Région Limousin. We gratefully acknowledge Wolfgang Sohler for many helpful and stimulating discussions. Our thanks go also to A. Dexet for the development and his advices for all the specific mechanical components.


## REFERENCES


Boyd R. W., 1990, Nonlinear Optics, 3rd edn. Academic Press, New York

Brustlein S., Del Rio L., Tonello A., Delage L., Reynaud F., Herrmann H., Sohler W., 2008, Phys. Rev. Lett., 100, 153903

Büchter K.-D. F., Herrmann H., Sohler W., 2011, in Advanced Photonics, Waveguide-based Mid-Infrared Up-conversion Detectors. Optical Society of America, p. IWF3,

Gomes J.-T. et al., 2014, Phys. Rev. Lett., 112, 143904

Gräfe C., Wolf S., 2013, A&A, 552, A88

Lopez B. et al., 2009, Proc. SPIE Conf. Ser., SPIE, Bellingham, p. 1, available at (http://hal.archives-ouvertes.fr/hal-00335606)

Louisell W. H., Yariv A., Siegman A. E., 1961, Phys. Rev., 124, 1646

Perrin G., Leinert C., Graser U., Waters L. B. F. M., Lopez B., 2001, CR Acad. Sci., Paris IV, 2, 79


This paper has been typeset from a TEX/LATEX file prepared by the author.